

RESEARCH ARTICLE

Numerical and on-site assessment of RC slab behavior in a multistory building under various loading combinations

Barış Güneş¹, Turgay Coşgun¹, Kamran Samadi², Turhan Bilir¹, Barış Sayın¹

- ¹ Istanbul University-Cerrahpaşa, Department of Civil Engineering, Istanbul, Türkiye
- ² Istanbul University-Cerrahpaşa, Institute of Graduate Sciences, Istanbul, Türkiye

Article History

Received 21 April 2024 Accepted 14 November 2024

Keywords

Deflection control Slab deflection Cracking RC slab Deformation Serviceability

Abstract

This study investigates slab damage, the underlying causes of these damages, and the post-damage performance of a five-story reinforced concrete building with shear walls under construction. Deflections and visible cracks resulting from these deflections were observed in the slabs and beams of the building under investigation. To assess the risk and progression potential of the existing damage, the vertical structural elements in the 1st normal floor of the building and the beams and slabs in the ceiling were modeled in Midas Gen finite element software. This model was subjected to the loads from structural elements, construction loads, coating loads, material loads intended to correct the existing slab slope, and live loads. Additionally, an in-situ loading test was conducted to evaluate the post-damage performance of the slabs under vertical loads, and this test was incorporated into the numerical analysis. To represent the structure's behavior under loads during the construction process, the time-dependent change in concrete strength was considered. For the cracked section analysis of the slabs, the EN 1992-1-1 standard was considered, and cracked section stiffness was applied for each mesh element representing the slab. When cracking occurred, the effective moment of inertia was calculated in both directions, and displacements for the cracked section were determined based on this moment of inertia. The analysis model contains approximately 3,000 meshes representing the slabs. Instead of employing a single effective moment of inertia for the entire slab, the effective moment of inertia is calculated separately for each mesh segment. The analyses, which considered five different load combinations, revealed that the slab displacements in service conditions exceeded the limit values specified in the applicable codes, indicating that the slabs require strengthening.

1. Introduction

The serviceability of a building is related to the absence of excessive deflection and cracks in its structural element. Put another way, deflections must be controlled to ensure safety and serviceability in reinforced concrete (RC) structures. Therefore, the calculation of slab deflections, as well as the consideration of creep

eISSN 2630-5763 © 2023 Authors. Publishing services by golden light publishing®.

^{*} Corresponding author (<u>barsayin@iuc.edu.tr</u>)

This is an open-access article under the CC BY-NC-ND license (http://creativecommons.org/licenses/by-nc-nd/4.0/).

and shrinkage effects, is necessary [1]. Consequently, adherence to the span-to-depth ratios prescribed in the codes or conducting deflection calculations becomes essential for effective deflection control [2].

Numerous studies have explored slab behaviors. For example, Reda Taha and Hassanain [3] argued that design regulations are inadequate in some cases, especially in deflection-sensitive elements such as floor slabs, and that calculated deflection values can be significantly lower than the actual deflections observed. The authors introduced a mathematical model using error propagation theory to estimate the error in the calculated deflection for simply supported one-way reinforced concrete slabs. In another study, Muthu et al. [4] examined partially restrained slab strips and proposed an analytical method to predict the load-deflection behavior of these strips. Their results indicated that higher load-carrying capability can be achieved by using less steel ratio, steel with less yield strength, higher edge stiffness, and higher concrete strength. Marí et al. [5] proposed a simplified method for calculating permanent deflections, which incorporates fundamental parameters reflecting the time-dependent behavior of reinforced concrete sections and members. The implementation of their method revealed that including the creep coefficient and shrinkage stress in the simplified formulas is essential for accurately estimating delayed deflections at any point during the service life of normal or high-strength concrete structures. Gilbert [6] examined the impacts of creep and shrinkage on the deflection and cracking of RC beams and slabs. The author introduced equations for calculating both instantaneous and permanent deflections. Scanlon and Suprenant [7] proposed a simplified calculation method for predicting deflections in two-way slabs in multi-story buildings, accounting for loading history, time-dependent concrete properties, and the effects of cracking. Their results indicated that the 28-day compressive strength predictions generated by the method aligned reasonably well with the experimental results obtained from test slabs. Caldentey et al. [8] introduced a new formulation for slenderness limits in the deflection control of RC flexural members, which was found to be compatible with the EN 1992-1-1 code [9]. Motter and Scanlon [10] developed an analytical algorithm to compute the center panel deflection history of RC two-way slabs in multistory buildings. Their results revealed that the center panel slab deflections estimated by the model were more responsive to alterations in slab thickness and aspect ratio compared to variations in the construction scheme. Kilpatrick and Gilbert [11] argued that AS3600-2009 [12] tends to underestimate short-term deflection, particularly for lightly reinforced concrete slabs. They suggested using the approach provided in EN 1992-1-1 [9] for a more realistic estimation. In addition, utilizing a coefficient or conducting separate calculations for shrinkage and creep deflections was recommended for a further accurate deflection calculation. Mari et al. [13] developed slenderness limits for deflection control and proposed a new formula. They validated the accuracy of these limits by comparing results from a nonlinear time-dependent analysis with those from permanent deflection calculations based on Eurocode 2. Eren and Dancygier [14] examined simplified methods based on span-to-depth ratios as outlined in the EN 1992-1-1 [9] and SII [15] codes. They found that both simplified approaches closely align with deflection measurements for slabs. However, for beams, they concluded that the SII [15] method, which incorporates more conservative ACI [16] data, shows greater consistency than EN 1992-1-1 [9]. Hasan and Taha [17] examined the effects of aspect ratio (long span/short span), concrete strength class, and live load on the permanent deflection of joistless floor panels. They noted that the aspect ratio is often overlooked in permanent deflection calculations in existing regulations. Their findings indicated that ACI 318-14 requirements are generally adequate for meeting the L/360 thickness limit for plain slabs without beams and the L/240 limit for typical spans and concrete strength classes. However, they found that these requirements are frequently insufficient for achieving the L/480 limit. Tosic et al. [18] proposed a practical method for controlling the deflection of bidirectional reinforced concrete slabs. This method utilizes elastic deflections from linear elastic analysis in finite element software, yielding results that align well with experimental data in the literature and demonstrate satisfactory precision and accuracy. Hu et al. [19] proposed a formula for calculating the deflection of a reversible aggregate bidirectional concrete slab. They compared the values obtained from this formula with those from an existing theoretical formula, calculated a correction coefficient for deflection, and validated the accuracy of this coefficient using data from model testing. Loewe et al. [20] developed a new method that optimizes existing approaches to facilitate the design of slabs with appropriate depth. This method is independent of the slab's reinforcement ratio, unlike the Eurocode 2 approach. Additionally, it accounts for multiple factors affecting slab depth-including span, load, allowable deflection, incremental deflection, and concrete's modulus of elasticity—unlike ACI 318 and Eurocode 2. Considering the importance of span-to-depth ratio limits for deflection control in the design of reinforced concrete structures, Santos and Henriques [21] established new span-to-depth ratio limits for reinforced concrete continuous beams and slabs, informed by the MC2010 [22] and EN 1992-1-1 [9] codes. They found that the newly proposed span-to-depth ratio limits meet both ductility and deflection requirements and are influenced by several factors, including the redistribution factor, the characteristic compressive strength of concrete, and the total reinforcement ratio. Priyanka and Ramesh [23] conducted an analytical and experimental comparison of slab deflections, both with and without a magnification coefficient, to assess the accuracy of Rankine-Grashoff and Timoshenko's plate theories. They found that the theoretical values for one-way slabs differed from the experimental values by 45%, while the theoretical values for two-way slabs were in good agreement with the experimental results. Sun et al. [24] proposed a crack detection method utilizing graph-based anomaly calculations to monitor the condition of concrete slabs in high-speed railroad tracks. Compared to other detection methods, their approach demonstrated success with minimal or no need for core samples. Pecic et al. [25] proposed a span-to-depth ratio procedure for deflection control in one-way reinforced concrete slabs and rectangular reinforced concrete beams. This procedure accounts for the effects of cross-sectional dimensions, the area and placement of tensile and compressive reinforcement, material properties, and the permanent creep and shrinkage parameters of concrete. The proposed procedure was validated through numerous numerical simulations utilizing various input combinations for deflection control and design. Derdiman [26] employed a Particle Swarm Optimization (PSO) algorithm to develop models that comply with TS500 [2] criteria for various slabs with beams running in two directions and having diverse dimensions. The researcher determined the optimal section and reinforcement bar (rebar) ratio for different slab configurations. Vecchi et al. [27] examined the long-term effects of creep and shrinkage on a reinforced concrete slab utilizing the PARC CL 2.1 [28] crack model. Their findings indicated that employing MC2010 [22] formulations for time-dependent behaviors of concrete often leads to an overestimation of the slab's long-term deformations. Sakic et al. [29] examined the impact of slab deflection on the out-of-plane capacity of masonry walls. Their findings indicate that slab deflection can cause significant damage or substantially reduce the out-of-plane capacity of these walls. Ravasini et al. [30] examined the impacts of concrete creep and shrinkage for nonlinear analysis in RC slabs using a finite element model, taking into account serviceability limits. Their findings revealed that permanent deflection is influenced by various factors including the modulus of elasticity and strength of concrete, creep, shrinkage, the ratios of hogging and sagging reinforcements, the effective depth/total depth ratio of the slab, and environmental conditions. Ahmed et al. [31] conducted analytical and experimental investigations into the impact of carbon and steel plates on the flexural strength of RC slabs with varying thicknesses. Their results suggested that steel plates are more effective than carbon plates in reinforcing RC slabs and result in a greater reduction of deflections. El-Ashmawy and El Zareef [32] proposed an innovative and efficient method for detecting structural displacements, utilizing a least squares solution to generate a concurrent solution that incorporates all observed data in a single process. They found that the proposed mathematical method outperforms established approaches in the literature, including ACI 318-19, in terms of accuracy, applicability, time savings, and cost-effectiveness in assessing structural element deformation.

As discussed above, although many studies have examined slab behaviors, only a limited number of studies have conducted on-site slab loading tests considering different scenarios. Accordingly, this study

aimed to assess slab behaviors through both numerical simulations and on-site evaluations. A representative slab identified as critical was modeled and analyzed using finite element software to evaluate potential damages in a five-story shear-reinforced concrete building during construction. Additionally, on-site observations and a loading test were performed. The results obtained from the analysis of this slab were used to predict the behavior of all slabs within the structural system and to assess all slab damage. Furthermore, the outcomes of the numerical model were compared with on-site measurements, and potential reasons for discrepancies were discussed. The novelty of this study lies in determining the damage distribution and experimentally investigating the post-damage behavior in a full-scale real structure. This approach allows for a better understanding of the slab's performance under vertical loads, which has not been extensively addressed in previous studies. We believe these findings will make a valuable contribution to existing literature.

2. The building examined

The building under construction, where slab damages were analyzed, features a reinforced concrete (RC) frame and shear wall structural system. It comprises three basement floors, a ground floor, first and second normal floors, and an attic floor. The building exhibits generally regular geometry, with dimensions of 40.2 meters in the x-direction and 16.9 meters in the y-direction at the ground floor level. The total floor area of the ground floor is 677 square meters. The floor heights are 4.1 meters on the ground floor, 3.6 meters on the first and second floors, and 5.3 meters in the attic. In the construction of the building, C30 class concrete and S420 class rebar were used.

2.1. Slab characteristics

Tables 1 and 2 present the rebar arrangements and current deflections in the building's slabs obtained during on-site examinations.

Table 1. Rebar arrangements in the slabs

Floor	Slab Thickness (cm)	Lower and Upper Rebars	Additional Rebar	Stirrup
3 rd Basement	15 and 30	Ø10 and Ø12 @ 15~20 cm	Ø10, Ø14, and Ø20 @ 15~20 cm	Ø12 and Ø14 @15 cm
2 nd Basement	15 and 30	Ø10 and Ø12 @ 15~20 cm	Ø10, Ø14, and Ø20 @ 15~20 cm	Ø12 and Ø14 @15 cm
1st Basement	15 and 30	Ø10 and Ø12 @ 15~20 cm	Ø10 and Ø20 @ 15~20 cm	Ø12 and Ø14 @15 cm
Ground	15 and 30	Ø10 and Ø12 @ 15~20 cm	Ø10 and Ø20 @ 15~20 cm	Ø12 and Ø14 @15 cm
2 nd Normal	15 and 30	Ø10 and Ø12 @ 15~20cm.	Ø10 and Ø20 @ 15~20 cm	Ø12 and Ø14 @15 cm
1 st Normal	15 and 30	Ø10 and Ø12 @ 15~20 cm	Ø10 and Ø20 @ 15~20 cm	Ø12 and Ø14 @15 cm
Attic	15	Ø10 and Ø12 @ 15 cm	Ø12 @ 15~30 cm	Ø12 and Ø14 @15 cm

Table 2. Current deflections in the slabs

Floor	Deflection			
rioor	Slab 1 (cm)	Slab 2 (cm)	Slab 3 (cm)	Slab 4 (cm)
3 rd Basement	4.7	5.0	4.6	1.0
2 nd Basement	5.6	4.9	6.7	5.5
1st Basement	6.0	2.5	5.0	5.0
Ground	3.6	4.2	-	-
1st Normal	7.0	3.2	-	-

2.2. Damage assessment

Deflections and visible cracks resulting from these deflections were observed in the slabs and beams of the building under investigation. Fig. 1 shows images of these damages. As expected, cracks appeared in the section of the slab located between the stairwells, running perpendicular to the long axis of the gap. However, beyond the stairwell sections, the cracks gradually shifted direction, aligning parallel to the long axis of the gap.

2.3. On-site investigations, loading setup

During the on-site investigations, a unit area test load of 8.5 kN/m² was applied to a 30 cm thick floor slab at the ceiling of the first normal floor of the building. The loading configuration and the approximate application area are shown in Fig. 2. The loading was maintained for two weeks. During this period, the vertical displacement of the slab measured approximately 12 mm. Following the removal of the load, most of the vertical displacement was recovered, and no permanent displacement was observed.

Numerical analyses

3.1. Modeling the load-bearing system

The analysis model created for the slab analysis is shown in Fig. 3. All vertical structural components of the first floor, as well as the beams and slabs comprising the ceiling of this floor, were included in the model. In the finite element program, plate elements with six degrees of freedom were used to model the shear walls and slabs, while beam-column elements with six degrees of freedom were utilized for the beams. The analysis model comprises reinforced concrete (RC) shear walls with thicknesses of 25 cm and 30 cm, RC beams with dimensions of 25×60 cm, 30×60 cm, 30×80 cm, 40×60 cm, and 50×60 cm, and RC slabs with thicknesses of 15 cm and 30 cm. Boundary conditions with varying degrees of freedom were defined at the wall-slab joints and shear wall edges. The first floor was modeled because it exhibits the most significant damage and is the most critical in terms of the structural system (with no basement walls), representing the overall structure. It is believed that the calculations made for this floor regarding the cause of the damage will represent the building. The mesh placement and dimensions were created according to the regions where slab sizes and reinforcements varied. No convergence study was performed by altering the mesh sizes; instead, a single mesh system was utilized with a high number of small mesh sizes. This approach is expected to be sufficient to reflect the general behavior of the structure. As shown in Fig. 4, rotational freedom was defined for the edges of shear walls at the shear wall-slab joints, assuming that rotation at these points was permitted. Fig. 5 illustrates the rebars used in the slabs. The top and bottom rebars, additional rebars, and stirrups were delineated separately within the analysis model. Fig. 5 illustrates the rebars used in the slabs. The top and bottom rebars, additional rebars, and stirrups were delineated separately within the analysis model.



Fig. 1. Slab damages

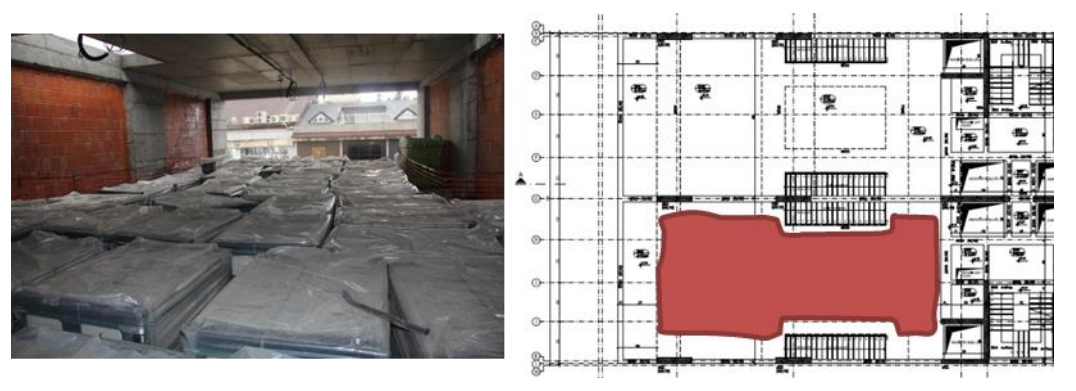


Fig. 2. On-site loading test and application area

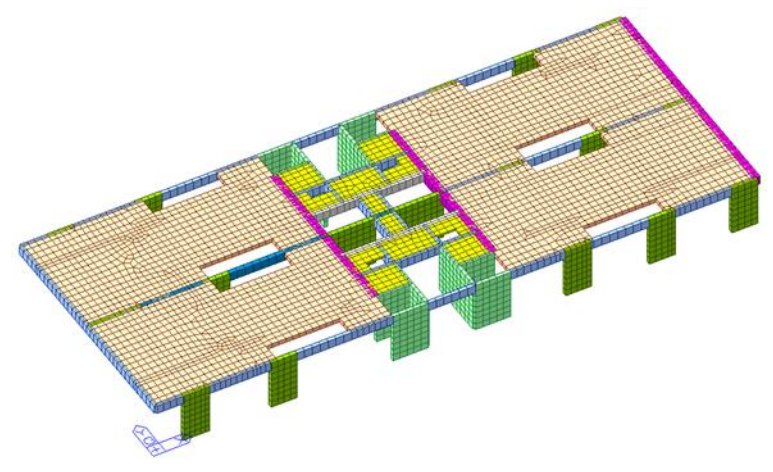


Fig. 3. The analysis model for 1st normal floor

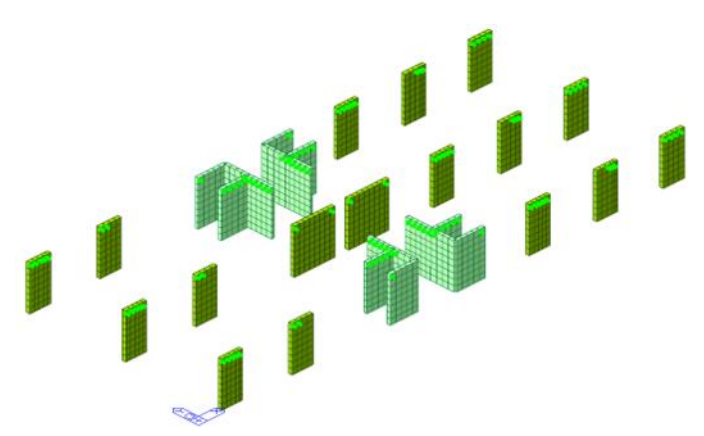


Fig. 4. Freedom of rotation at shear wall-slab joints

3.2. Loads considered in analysis

For slab analysis, the external effects (dead, live, and test loads), to which a structure is exposed during its construction, erection, and utilization were identified. The self-weight of the structural elements was defined as the dead load (D1), with the unit weight of reinforced concrete set at 25 kN/m³. In accordance with the construction stages, the slab was subjected to the weight of the formwork, as well as the weight of the slab from the floor above. This load was taken as 8.5 kN/m² (C1), comprising 7.5 kN/m² for the weight of fresh concrete and 1.0 kN/m² for the weight of formwork. (D1a). Non-structural elements (such as coatings, marbles, leveling concrete, and flooring), which are not included in the finite element program, were defined as dead loads (D2) corresponding to their self-weight. As provided in the statical project, the D2 loading was set at 2.1 kN/m². The live load (L1) is defined as non-permanent loading conditions that temporarily act on structural elements. Therefore, a live load of 5 kN/m² was defined, in accordance with the structural design specifications, to represent the live loads that the structure will experience during its service life after construction. During on-site investigations, a test load of 8.5 kN/m² (T1) was applied by placing weight on a specific slab section. Considering the losses incurred due to the load application practice, this load was multiplied by a coefficient of 0.75 and defined as 6.5 kN/m² in the model.

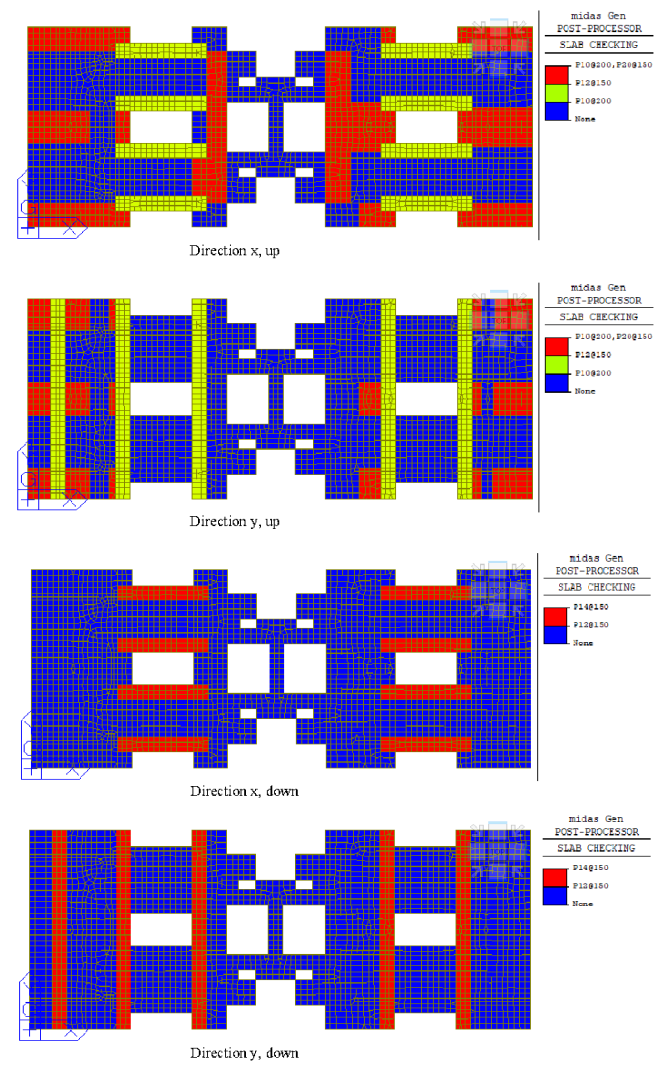


Fig. 5. Slab rebars

3.3. Defining material properties

In the static project, the concrete class used in the building was specified as C30/37, and the rebar class was defined as S420. Accordingly, the final strength of the concrete cylinder and the yield strength of the rebars were established as 30 MPa and 420 MPa, respectively. However, damages observed in the slabs occurred during manufacturing rather than at final stages. Therefore, different concrete strengths were defined corresponding to various manufacturing stages and loading conditions, as shown in Table 3. Since the existing conditions were examined rather than the design, the concrete and rebar strengths were defined without applying the material safety coefficients of 1.5 and 1.15 outlined in TBEC 2018 [33]. The Mander concrete model [34] was utilized to simulate concrete behavior, and the modulus of elasticity was calculated using Eq. 1.

$$E = 5000\sqrt{fc} \tag{1}$$

Manufacturing Stage	Loading	Concrete Compressive Strength, MPa	Modulus of Elasticity of Concrete, MPa	Yield Strength of Rebar, MPa
Stage-1	D1, ~7 days	16	20000	420
Stage-2	C1, ~15 days	25	25000	420
Stage-3	D1a, D2, L1, T1, 28 days	30	27386	420

Table 3. Material strengths for different manufacturing stages and loading conditions

D1: Dead Loads, C1: Construction Loads, D1a: Weight of the Formwork, D2: Non-Structural Element Loads,

L1: Live Load, T1: Test Load

3.4. Analysis method for cracked slabs

The examined slab was modeled on the Midas Gen [35] finite element program and cracked section analysis was performed according to the EN 1992-1-1 [9] standard. In this modeling approach, the slab was not simplified to a beam or bar; instead, each mesh representing the slab was examined for cracking in accordance with the applicable codes. If cracking was identified, the effective moment of inertia was calculated for both directions, and displacements were determined for the cracked section using this moment of inertia. Accordingly, the analyses were performed iteratively. The model included approximately 3,000 meshes representing the slabs. These calculations were repeated for each mesh until the specified iteration tolerance was met. The aim was to achieve the most realistic behavior possible, accurately representing the actual situation. Rather than employing a single effective moment of inertia for the entire slab, the effective moment of inertia was computed and applied to each component separately. Second-order effects and the nonlinear behavior of the material were not considered in the analysis. However, more precise and realistic results could be obtained by accounting for these effects, but this is beyond the scope of the current study.

4. Results and discussion

Details of the loading for the examined slab are provided in Table 4. Displacement analyses were conducted separately for the cracked sections considering five different cases. Initially, Case-1 was investigated based on the observation that cracks and deflection occurred even under the slab's own weight. Subsequently, Case-2 was analyzed, representing the actual cracks and damages observed. It was assumed that the cracks and vertical displacements occurring during Case-2 were permanent. Even after the removal of the manufacturing loads (C1), the resulting displacements (Δ C1) were assumed to remain permanent. Case-3 was examined for short-term final displacement in the slab during service. To assess the long-term displacement in the slab, Case-4 was investigated by applying half of the live loads in the calculations, as prescribed by the applicable code. To represent the on-site test conditions, Case-5 was examined. Although there was no C1 loading in Case-3, Case-4, and Case-5, the permanent deflections, cracks, and moments of inertia reduction resulting from C1 (Δ C1) were incorporated into the displacement analysis with certain assumptions.

Table 4. Examined loading scenarios for slab analysis

Case	Loading	Duration
1	D1	7 days
2	D1 + C1	12~15 days
3	$D1 + \Delta C1 + D1a + D2 + L1$	28 days
4	$D1c + \Delta C1 + D1ac + D2c + 0.5L1c$	Long-term
5	$D1 + \Delta C1 + T1$	28 days

4.1. Analysis results for Scenario-1

Fig. 6 illustrates the displacements for uncracked and cracked sections of the slab in Scenario-1. The displacement resulting from the reduction in the moment of inertia due to cracking in the slab was nearly double that of the uncracked section. The displacement observed in the uncracked condition was 7.16 mm, which increased to 13.74 mm in the cracked section. According to the effective moment of inertia approach outlined in EN 1992-1-1 [9], the effective moment of inertia ratio in the y-direction, where cracking is anticipated, was multiplied by a factor of 0.34, while in the x-direction, where cracking is not anticipated, it was multiplied by a factor of 1.00. This increase in displacement indicates that cracks can occur in the slab even under dead load alone due to the assumptions made.

4.2. Analysis results for Scenario-2

Displacements in the cracked section of the slab for Scenario-2 are shown in Fig. 7. The displacement resulting from the reduction in the moment of inertia due to cracking in the slab was 45.55 mm. According to the effective moment of inertia approach outlined in EN 1992-1-1 [9], the effective moment of inertia ratio in the y-direction, where cracking is anticipated, was multiplied by a factor of 0.34, while in the x-direction, where cracking is not anticipated, it was multiplied by a factor of 1.00. The resulting displacement indicates that numerous cracks occur in the slab under the dead loads, fresh concrete load, and formwork load due to the assumptions made.

4.3. Analysis results for Scenario-3

Fig. 8 illustrates the displacements for cracked sections of the slab for Scenario-3. The displacement caused by the reduction in the moment of inertia due to cracking in the slab was measured at 76.00 mm. According to the effective moment of inertia approach detailed in EN 1992-1-1 [9], the effective moment of inertia ratio in the y-direction, where cracking is expected, was multiplied by a factor of 0.34. In contrast, in the x-direction, where cracking is not anticipated, it was multiplied by a factor of 1.00. The observed displacement indicates that numerous cracks occur in the slab under the dead loads, coating loads, and live loads based on the assumptions. Although no C1 loading was applied in Case-3, permanent deflections and cracks resulting from C1 were incorporated into the total displacement under certain assumptions.

4.4. Analysis results for Scenario-4

For long-term deflection analysis, the creep coefficient was taken as 3. The deflection of the slab at the manufacturing stage (Scenario-2, D1+ Δ C1) was calculated to be approximately 45 mm. The additional long-term deflection due to the D1 loading was estimated at approximately 35 mm (D1c - D1, 49 - 14 = 35 mm). Conversely, the long-term deflection due to the D1ac + D2c + 0.5 × L1c loading was calculated to be 85 mm. Accordingly, the estimated long-term deflection in the slab was 165 mm (45 + 35 + 85). Considering that the C1 loading is not long-term, no additional long-term deflection was anticipated. However, permanent cracks and the reduction in moments of inertia resulting from this loading were considered

4.5. Analysis results for Scenario-5

Fig. 8 illustrates the displacements for cracked sections of the slab for Scenario-5. The displacement caused by the reduction in moment of inertia due to the cracks in the slab measured 73 mm. The initial deflection of the slab due to manufacturing (Scenario-2, D1 + Δ C1) was estimated to be around 45 mm. Therefore, the displacement attributed to the test loading was determined to be 28 mm (73 - 45). The displacement recorded during on-site examinations under T1 loading was 18 mm. This variance is attributed to the concrete strength being higher than C30 at the time of testing, as well as the approximate load value. Although there was no

C1 loading in Scenario-5, permanent deflections (Δ C1), cracks, and the reduction in moment of inertia resulting from C1 loading were considered in the calculations based on the assumptions made.

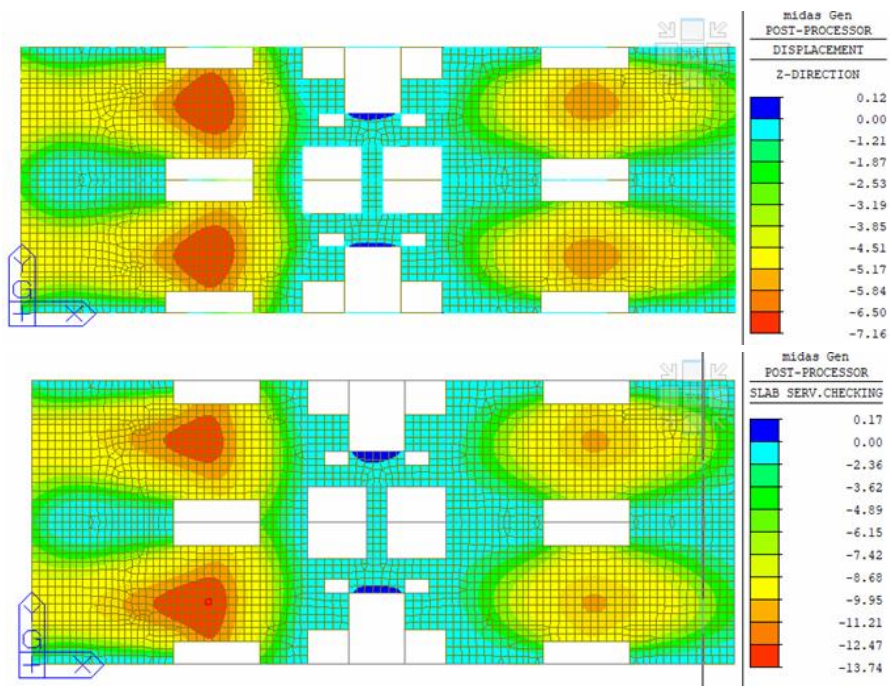


Fig. 6. Scenario-1 (D1 loading): Displacements for uncracked (top) and cracked (bottom) sections of the slab

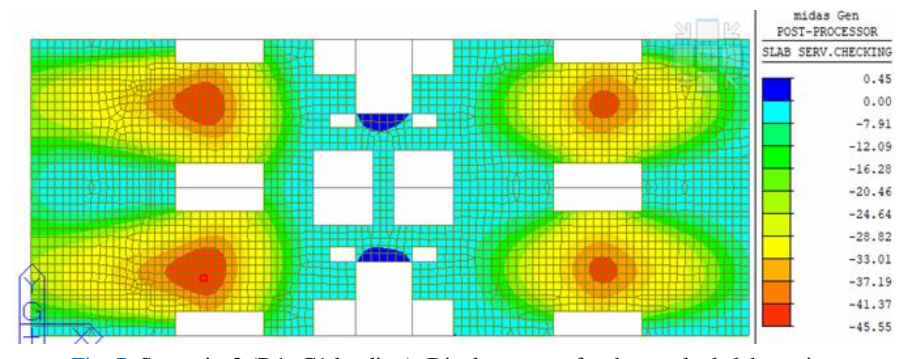


Fig. 7. Scenario-2 (D1+C1 loading): Displacements for the cracked slab section

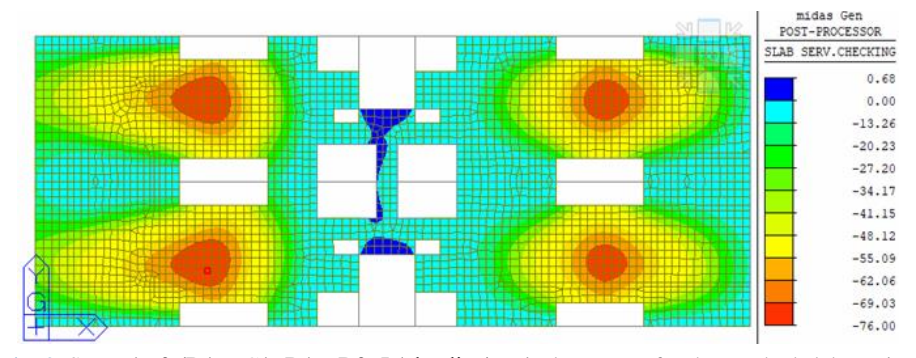


Fig. 8. Scenario-3 (D1+ΔC1+D1a+D2+L1 loading): Displacements for the cracked slab section

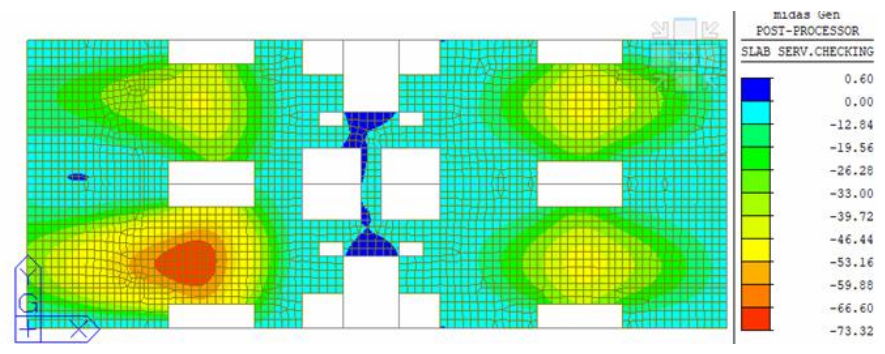


Fig. 9. Scenario-5 (D1+ Δ C1+T1 loading): Displacements for the cracked slab section

Table 5. Displacements obtained from slab analyses

Scenario	Loading	Displacement, mm
1	D1	13.74
2	D1 + C1	45.55
3	$D1 + \Delta C1 + D1a + D2 + L1$	76.00
4	$D1c + \Delta C1 + D1ac + D2c + 0.5L1c$ (c: creep, long-term deflection)	≈165
5	$D1 + \Delta C1 + T1$	73.32

4.6. Overall results

The examined cases and results are summarized in Table 5. First, the slab was evaluated considering only its self-weight (Scenario-1). Subsequently, Scenario-2, representing the formation of the existing cracks and damages during the manufacturing phase, was analyzed. The cracks and vertical displacement observed in Scenario-2 were assumed to be permanent. Even though the manufacturing loads (C1) were removed, the displacements caused by these loads (Δ C1) were considered permanent. To determine the long-term final displacement of the slab in service, Scenario-3 was examined. Scenario-4 analyzed the long-term displacements of the slab by applying half of the live loads as stipulated in the applicable code. To simulate the on-site loading test, Scenario-5 was evaluated. Despite the absence of C1 loading in Scenarios 3, 4, and 5, the permanent deflections, cracks, and moment of inertia reductions resulting from C1 (Δ C1) were included in the displacement calculations through certain assumptions. The displacements of the slab in the service condition were found to exceed the limit value of L/480.

5. Conclusions

To analyze and evaluate slab damages in the RC building under construction, a finite element model of a critical slab section was developed and examined. The results obtained from the model were compared with those from on-site loading tests. The key findings of the study are summarized below:

- During on-site inspections, deflections were observed in several RC slabs and beams, accompanied
 by cracks resulting from these deflections. As anticipated, cracks formed in the section of the slab
 located between the stairwells, running perpendicular to the long axis of the gap. In contrast, in
 other sections, the cracks gradually changed direction, aligning parallel to the long axis of the gap.
- Cracked section analysis was performed for the examined slab. Each mesh representing the slab
 section was numerically evaluated for crack formation. If cracking was detected, the effective
 moment of inertia was calculated for both directions, and the displacements for the cracked section
 were determined using this moment of inertia. Rather than using a single effective moment of inertia

for the entire slab, the effective moment of inertia for each component was calculated and applied separately. As expected, some slab sections exhibited cracks while others did not. This methodology aims to achieve the most realistic behavior possible, accurately reflecting the actual conditions.

- The analyses, which considered five different load combinations, revealed that the slab displacements in service conditions exceeded the limit values specified in the applicable codes, indicating that the slabs require strengthening.
- Some variations were observed between the displacements obtained from the cracked section
 analyses and those measured during on-site examinations. While the displacement calculated for
 the manufacturing phase was 45 mm, the in-situ measured value was approximately 50–60 mm.
 Possible reasons for this difference include defects in the slab formwork, measurement errors in the
 field, disparities in concrete and reinforcement strengths, inconsistencies in rebar diameters and
 spacing between the project specifications and construction, and variations in boundary conditions.
- Despite the proper preparation and leveling of the formworks during fabrication, it was observed
 that the lower floor slab, which was subjected to the weight of fresh concrete and formwork and
 had not yet attained the anticipated concrete strength outlined in the project, experienced greater
 displacement than expected. Consequently, permanent deflection was noted in the slab. Therefore,
 it is believed that a significant portion of the variation between the numerically calculated and actual
 displacements may be attributed to this behavior.

As a result, the analysis of potential short- and long-term displacements and their distribution throughout the structure for different scenarios (Scenarios 1-5) indicated that the current strength of the slabs is inadequate and requires appropriate strengthening. This study is believed to contribute to literature by demonstrating the importance of considering the loads and potential permanent deflections during the manufacturing phase in the design and analysis of reinforced concrete slabs. Future studies may consider second-order effects and nonlinear material behavior for more precise and realistic results. Performing similar analyses on different structures may also provide more generalizable insights.

Conflict of interests

The author(s) declared no potential conflicts of interest with respect to the research, authorship, and/or publication of this article.

Funding

This research received no external funding.

Data availability statement

Data generated during the current study is available from the corresponding author upon reasonable request.

References

- Cope RJ, Clark LA (1984) Concrete slabs: Analysis and design. Taylor & Francis, New York, ISBN: 0-85334-254-7
- TS500: Requirements for Design and Construction of Reinforced Concrete Structures, Turkish Standards Institute, Ankara.
- [3] Reda Taha MM, Hassanain MA (2003) Estimating the error in calculated deflections of HPC slabs: a parametric study using the theory of error propagation. Special Publication 210:65-92.
- [4] Muthua KU, Amarnatha K, Ibrahim A, Mattarneh H (2007) Load deflection behaviour of partially restrained slab strips. Engineering Structures 29:663–674.

[5] Marí AR, Bairan JM, Duarte N (2010) Long-term deflections in cracked reinforced concrete flexural members. Engineering Structures 32:829–842.

- [6] Gilbert RI (2011) The serviceability limit states in reinforced concrete design. Procedia Engineering: 14, 385–395.
- [7] Scanlon A, Suprenant B (2011) Estimating two-way slab deflections. Concr. Int. 33(7):29–34.
- [8] Caldentey AP, Cembranos JM, Peiretti HC (2016) Slenderness limits for deflection control: A new formulation for flexural reinforced concrete elements. structural concrete 18:118–127.
- [9] EN 1992-1-1. Eurocode 2: Design of Concrete Structures Part 1-1: General Rules and Rules for Buildings. European Committee for Standardization, Brussels, Belgium, 2004.
- [10] Motter CJ, Scanlon A (2018) Modeling of reinforced concrete two-way floor slab deflections due to construction loading. Struct Eng 144(6).
- [11] Kilpatricka AE, Gilbert RI (2018) Simplified calculation of the long-term deflection of reinforced concrete flexural members. Australian Journal of Structural Engineering 19(1):34–43.
- [12] AS3600-2009. Australian Standard for Concrete Structures, Standards Australia, Sydney, 2009.
- [13] Marí A, Torres L, Oller E, Barris C (2019) Performance-based slenderness limits for deformations and crack control of reinforced concrete flexural members. Engineering Structures 187:267-279.
- [14] Erena T, Dancygier AN (2020) Evaluation of span-to-depth ratio provisions for deflection control of one-way RC construction. Structures 25:696–707.
- [15] SII 466. Concrete Code: General Principles. The Standards Institution of Israel, 2003. (in Hebrew).
- [16] ACI 318-14. Building Code Requirements for Structural Concrete and Commentary. American Concrete Institute, ACI 318, Farmington Hills, 2014.
- [17] Hasan SA, Taha BO (2020) Aspect ratio consideration in flat plate concrete slab deflection. ZANCO Journal of Pure and Applied Sciences 32(5):62-77.
- [18] Tošic N, Pecic N, Poliotti M, Marí A, Torres L, Dragaš J (2021) Extension of the ζ-method for calculating deflections of two-way slabs based on linear elastic finite element analysis. International Federation for Structural Concrete 22:1652-1670.
- [19] Hu P, Fang G, Li Z (2021) Experimental study on deflection of recycled concrete two-way slab under concentrated load. IOP Conf. Series: Earth and Environmental Science 687.
- [20] Loewe MS, Llovera JC, Anaya SR, Gispert EP (2021) A path to more versatile code provisions for slab deflection control. Structures and Buildings.
- [21] Santos J, Henriques AA (2021) span-to-depth ratio limits for RC continuous beams and slabs based on MC2010 and EC2 ductility and deflection requirements. Engineering Structures 228.
- [22] fib Bulletin 56. Model Code 2010 First Complete Draft, Volume 2. Lausanne, Switzerland: International Federation for Structural Concrete (fib), 2010.
- [23] Priyanka MD, Ramesh V (2022) Comparative study on slab deflections. IOP Conf. Series: Earth and Environmental Science 982.
- [24] Sun W, Zhou Y, Xiang J, Chen B, Feng W (2022) Crack detection in concrete slabs by graph-based anomalies calculation. Smart Structures and Systems 29(3):421-431.
- [25] Pecic N, Mašovic S, Stošic S (2022) Span-to-depth ratio limits for deflection control of reinforced concrete elements. International Federation for Structural Concrete 1-16.
- [26] Derdiman MK (2022) reliability-based optimization of two-way RC slabs with beam under deflection constraint using discrete PSO algorithm. El-Cezerî Journal of Science and Engineering 9(1):49-64.
- [27] Vecchi F, Franceschini L, Belletti B (2022) PARC_CL 2.1: Modelling of the time-dependent behaviour of reinforced concrete slabs. Computational Modelling of Concrete and Concrete Structures.
- [28] Franceschini L, Vecchi F, Belletti B (2021) The PARC_CL 2.1 Crack model for NLFEA of reinforced concrete elements subjected to corrosion deterioration. Corrosion and Materials Degradation 2:474-492.
- [29] Sakic B, Marinkovic M, Butenweg C, Klinkel S (2023) Influence of slab deflection on the out-of-plane capacity of unreinforced masonry partition walls. Engineering Structures 276.
- [30] Ravasini S, Vecchi F, Belletti B, Muttoni A (2023) Verification of deflections and cracking of RC flat slabs with numerical and analytical approaches. Engineering Structures 284.
- [31] Ahmed SM, Ahmed SA, Abdulrahman PI (2023) Innovative approaches to deflection analysis in strengthened reinforced concrete slabs: Combining experiments and theoretical research. Structures 58.

- [32] El-Ashmawy KLA, El Zareef MA (2023) Dynamic monitoring of structural deformations utilizing an experimentally validated efficient technique. Engineering, Technology & Applied Science Research 13(3):10708-10713.
- [33] TBEC 2018. Turkey Building Seismic Code: Rules for Design of Buildings under Earthquake Effect. Official Gazette, Date: 18.03.2018, No: 30364 (in Turkish).
- [34] Mander JB, Priestley MJN, Park R (1988) Theoretical stress-strain model for confined concrete. Journal of Structural Engineering, ASCE 114(8):1804-1825.
- [35] Midas Gen (2021) Integrated Solution System for Building and General Structures. MIDAS Information Technology Co.